JOURNAL OF GUIDANCE, CONTROL, AND DYNAMICS
Vol. 31, No. 3, May–June 2008

Interplanetary Periodic Trajectories in Two-Planet Systems

Dmitry M. Pisarevsky*
Technion—Israel Institute of Technology, 32000 Haifa, Israel
Alexander Kogan†
Asher Space Research Institute, 32000 Haifa, Israel
and
Moshe Guelman‡
Technion—Israel Institute of Technology, 32000 Haifa, Israel

DOI: 10.2514/1.30046

A new technique is proposed to identify infinite families of candidate periodic trajectories (cyclers) in any restricted, coplanar, circular, two-planet system. In the simplest case in which only one of the planets enables gravity-assisted maneuvers, a method based on Hénon's diagram is used instead of solving Lambert's multiple-revolution problem. It provides the solutions in a comprehensible graphical form and suggests their natural classification. In the particular Earth–Mars case, it is shown that all previously found solutions for cyclers are present in Hénon's diagram. For the more general case in which both planets enable gravity-assisted maneuvers, Hénon's diagram is extended to present the trajectories that start and end near the same planet with the same relative velocity. This new extended diagram can be also used to predict periodic trajectories in this more general system. A discussion of all classes of periodic trajectories is presented.

Nomenclature

a	=	semimajor axis
e	=	eccentricity
F, G	=	Lagrange/Gibbs functions
$\mathbf{h}$	=	angular momentum vector
h	=	angular momentum magnitude
h_p	=	height of the hyperbola's pericenter
i	=	inclination angle
M_1, M_2, M_3	=	bodies in the three-body problem: central (sun), primary (planet), and spacecraft
m_1, m_2, m_3	=	masses of M_1, M_2, and M_3
m	=	number of spacecraft's semirevolutions
n	=	number of primary's semirevolutions
P1, P2	=	primary bodies (planets) in the four-body problem
p	=	semilatus rectum
$\mathbf{r}$	=	position vector
r	=	distance from the central body
T	=	orbital period
t	=	time
t_1, t_2, t_3, t_4	=	time intervals of legs 1, 2, 3, and 4
t_{13}	=	half-time interval of legs 1 and 3 ($2t_{13} = t_1 + t_3$)
T_{syn}	=	synodic period
$\mathbf{V}_2$	=	velocity vector of M_2
$\mathbf{V}_3$	=	velocity vector of M_3
$\mathbf{V}_\infty$	=	relative velocity vector
V_∞	=	relative velocity magnitude
Δt, Δf, ΔE	=	time, true anomaly, and eccentric anomaly intervals in Lagrange/Gibbs F and G functions
δ	=	deflection angle of relative velocity during flyby
ε, ε', ε''	=	binary parameters (± 1)
η	=	half-eccentric anomaly interval
θ	=	transfer angle
θ_1, θ_2, θ_3, θ_4	=	transfer-angle intervals of legs 1, 2, 3, and 4
θ_{13}	=	half-transfer-angle interval of legs 1 and 3 ($2\theta_3 = \theta_1 + \theta_3$)
μ	=	parameter in the three-body problem
μ_1	=	gravity constant of M_1
μ_2	=	gravity constant of M_2
ρ	=	radius of planet
τ	=	half-time interval
$\tilde{\tau}$	=	extended half-time interval

Subscripts

E	=	Earth
M	=	Mars

I. Introduction

PERIODIC trajectories, or *cyclers*, in two-planet systems are the trajectories that have periodical encounters with these planets. The concept of a cycler is not new. Several previous successful studies have shown that many such trajectories exist, both ballistic and powered. Using these trajectories, a cycler (a massive spacecraft) carries people or payload back and forth between two planets without stopping at either of them. In its turn, smaller space vehicles could ferry the load from one planet up to the cycler and from the cycler down to another planet, and vice versa.

The concept was first introduced in the late 1960s by Hollister [1], Menning [2], and Rall [3]. Ballistic cyclers in Earth–Mars and Earth–Venus systems were sought using nonlinear methods. Cycler interest was restarted in the mid-1980s and early 1990s following the discovery of Niehoff's Versatile International Station for Interplanetary Transport (VISIT) [4,5] cyclers and the Aldrin cycler [6]. More recently, several studies have indicated a continued interest in cyclers. In particular, these studies investigate Earth–Mars cyclers using Earth free-return trajectories patched together with gravity-assisted Earth flybys [7–10]. The free-return trajectories belong to three types: half-revolution $-(2k\text{-}1)\pi$ transfers, full-revolution $-2k\pi$ transfers, and generic transfers. Works performed by McConaghy et al. [7,8] found several cycler trajectories using a

Received 26 January 2007; revision received 21 November 2007; accepted for publication 22 November 2007.

*Doctoral Candidate, Faculty of Aerospace Engineering; aedmitry@techunix.technion.ac.il.

†Senior Scientist, Asher Space Research Institute; akogan@techunix.technion.ac.il.

‡Professor, Faculty of Aerospace Engineering; aerglmn@aerodyne.technion.ac.il. Senior Member AIAA.

single generic return trajectory and several cyclers using two identical or nonidentical generic returns patched by an Earth flyby. Byrnes et al. [9] showed that energy characteristics of a particular two-synodic-period cycler could be considerably improved by including half- and full-revolution returns. Patel et al. [10] proposed the use of Hénon's tables [11] to determine Earth–Mars free-return trajectories using generic arcs relative to Earth. Recent work by Russell and Ocampo [12–14] combined these approaches into one noniterative method that scans the defined solution space to identify and classify cycler orbits.

To our best knowledge, all previous works addressed the cyclers in planet systems in which only one of the planets (in our case, the Earth) is able to curve the spacecraft trajectory during a flyby, whereas the other (Mars) is not. In other words, Mars was assumed to be massless. This paper proposes an approach to the systems with both planets assumed to be massive. The cycler trajectory is assembled from the interplanetary transfers and, optionally, from several loitering arcs with both ends near the same planet. Generally, the angular distances of the loitering arcs are not restricted, but this paper is confined to the case in which the distances of all loitering arcs are the multiples of π. This set of arcs is sufficient to build a wide variety of periodic trajectories in any coplanar, circular, two-planet system.

The approach proposed in this paper is similar to that used by Hénon [11]. The major merits of Hénon's diagram are 1) explicit finite analytical equations, the same for all families of the sought orbits and 2) comprehensible presentation of the manifold of solutions naturally organized in physically distinctive families. These merits remain valid in the proposed method.

The fidelity of solutions available with the proposed technique is limited due to the simplified character of the mechanical model of the planetary system. This feature is characteristic of the great majority of studies in the field. However, the solutions can serve as first-guess approximations to exact trajectories. Of particular interest are the resulting cyclers that are entirely ballistic. Once set in orbit, ballistic cyclers use physically feasible flybys and require no powered maneuvers to maintain it.

II. Trajectories with Consecutive Collisions

We consider the trajectories with multiple gravity-assisted maneuvers in a system of a central body, two primaries, and a spacecraft. From those trajectories, we are interested in periodic trajectories. An approach we adhere to is splitting the trajectory into a sequence of three-body-problem (3BP) trajectories or, in a cruder approximation, into two-body-problem (2BP) trajectories.

A. Collisional Arcs

First, let us consider the case of three bodies: a central body, a primary body, and a spacecraft, all considered as material points moving in a space governed by Newton's gravitational law. Let their masses be $m_1 > m_2 \gg m_3$, respectively. In practice, m_3 is so small that its influence on the motion of the other bodies can be neglected, which means that $m_3 = 0$. This implies that the primary executes Keplerian motion around the central body. If we assume that the primary moves in a circle, the problem of the spacecraft motion is called the restricted circular 3BP. The so-called canonical scaling of time, length, and mass units [15] uses the primary orbital radius and inverse of the angular velocity as the length and time units, respectively, and $m_1 + m_2$ as the mass unit. The only remaining parameter is $\mu = m_2/(m_1 + m_2)$.

The 3BP may be further simplified when $\mu \ll 1$. The heliocentric spacecraft trajectory is nearly Keplerian everywhere except for a narrow vicinity of a primary. Here, the trajectory experiences a short impulse of attraction toward the primary, which curves the trajectory. When $\mu \to 0$ simultaneously with the flyby distance, the impulse duration tends to zero and the trajectory acquires a break, but relative velocities at arrival to and at departure from the primary are equal in modulus. The phenomenon looks like an ideally elastic collision, and so the asymptotic case under consideration is called, after Poincaré [16], the problem of trajectories with consecutive collisions. It deals with a chain of collisional trajectories [i.e., with Keplerian arcs having collisions at both ends (hereafter, just referred to as arcs or trajectories)].

B. Recursive and Transitional Arcs in the Four-Body Problem

Let us consider a system with a central body, two primaries, and a spacecraft. The primaries are presumed to move around the central body along the coplanar circular orbits. The masses of primaries are assumed to be small and their gravity interaction negligible, and so both primaries perform Keplerian motion around the central mass and their gravity spheres are infinitesimal. Therefore, the spacecraft motion obeys the patched conic model. Hereafter, we will refer to this model as to the restricted four-body problem (4BP).

We use *recursive* to denote the arcs that start and end near the same planet and *transitional* to denote those arcs that start and end near different planets. Furthermore, we split the recursive arcs in three families: *even*, *odd*, and *generic* arcs (see Fig. 1), and we split the transitional arcs into four families: *fast*, *slow*, *short*, and *long* arcs (see Fig. 2).

The naming of recursive arcs reflects the values of their transfer angles. In even arcs the transfer angle is $\theta = 2k\pi$; in odd arcs the transfer angle is $\theta = (2k-1)\pi$ (k is an integer); and generic arcs have any transfer angle, except those two sets of values (see Fig. 1). Note that even and odd arcs can be coplanar or out-of-plane, whereas generic arcs are always coplanar.

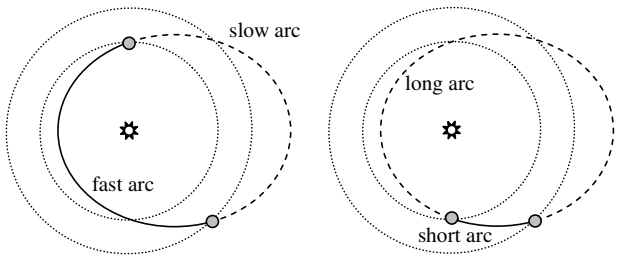

Fig. 2 Transitional arcs: a) fast and slow and b) short and long.

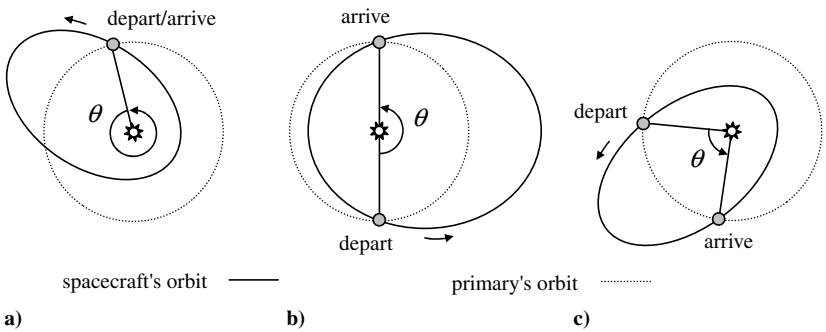

Fig. 1 Recursive arcs: a) even, b) odd, and c) generic arcs.

Table 1 Transitional arcs for $k \geq 0$

Arc type	Perihelion passages	Aphelion passages	Arc plane
Fast	$k+1$	k	Coplanar at $\theta \neq (2k+1)\pi$; coplanar or not at $\theta = (2k+1)\pi$
Slow	k	$k+1$	Coplanar at $\theta \neq (2k+1)\pi$; coplanar or not at $\theta = (2k+1)\pi$
Long	$k+1$	$k+1$	Coplanar
Short	k	k	Coplanar

The nomenclature of transitional arcs follows the same basic logic. Arc types differ in the perihelion/aphelion passage score, as shown in Table 1.

III. Periodic Trajectories in the Circular 3BP

A. Periodic Arcs

When omitting the constraint on the maximal turning angle of relative velocity, any arc with consecutive collisions in the restricted 3BP is a periodic trajectory. Hénon [11] gave an analytical approach to find these arcs. Unit length and time are canonical, and the collision points are denoted by Q_1 and Q_2 (see Fig. 3). Because the collision points are symmetrical with respect to the synodic X axis, it is sufficient to consider only half of the trajectory. The time interval between the collisions is 2τ; therefore, taking the middle of the interval as time $t = 0$, the collisions between the M_2 and the spacecraft M_3 occur at $-\tau$ and τ (see Fig. 3). In addition, at $t = 0$, both M_2 and M_3 are lying on axis X.

Assuming that the eccentric anomaly of the spacecraft is η at the time of collision, the synchronization condition can be written as a system of three equations [17], two equations for position (for the X and Y coordinates) and one equation for time (Kepler's equation):

$$\begin{cases} \cos\tau = \varepsilon a(\cos\eta - \varepsilon'' e) \\ \sin\tau = \varepsilon\varepsilon' a\sqrt{1-e^2}\sin\eta \\ \tau = a^{3/2}(\eta - \varepsilon'' e\sin\eta) \end{cases} \tag{1}$$

where a and e are the spacecraft semimajor axis and eccentricity, respectively, and parameters ε, ε', and ε'' describe different types of collisional orbits. Parameter ε describes initial position ($t = 0$) of M_2 and M_3 relative to M_1:

$$\varepsilon = \begin{cases} +1 \\ -1 \end{cases} \quad \text{if } M_2 \text{ and } M_3 \text{ at } t = 0 \begin{cases} \text{same} \\ \text{opposite} \end{cases} \text{side of } M_1$$

Parameter ε' defines the direct or retrograde motion of M_3:

$$\varepsilon' = \begin{cases} +1 \\ -1 \end{cases} \quad \text{if } M_3 \text{ orbit} \begin{cases} \text{direct} \\ \text{retrograde} \end{cases}$$

Parameter ε'' describes initial position ($t = 0$) of M_3:

$$\varepsilon'' = \begin{cases} +1 \\ -1 \end{cases} \quad \text{if } M_3 \text{ at } t = 0 \begin{cases} \text{periapsis} \\ \text{apoapsis} \end{cases}$$

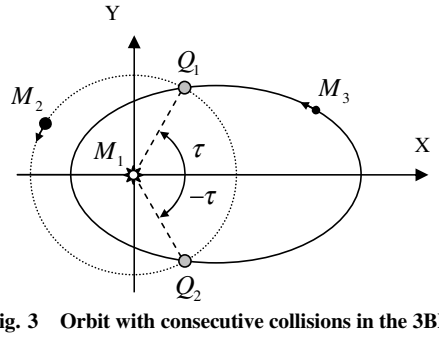

Fig. 3 Orbit with consecutive collisions in the 3BP.

From the first two equations of Eq. (1), we obtain

$$a = \frac{1 - \varepsilon\cos\tau\cos\eta}{\sin^2\eta} \tag{2}$$

$$e = \frac{\varepsilon''\cos\eta - \varepsilon\varepsilon''\cos\tau}{1 - \varepsilon\cos\tau\cos\eta} \tag{3}$$

Substituting Eqs. (2) and (3) into the third equation of Eq. (1), we obtain the implicit timing equation relating τ and η:

$$\sqrt{1 - \varepsilon\cos\tau\cos\eta}[\eta(1 - \varepsilon\cos\tau\cos\eta) - \sin\eta(\cos\eta - \varepsilon\cos\tau)] - \tau|\sin\eta|^3 = 0 \tag{4}$$

Hénon [11] solved Eq. (4) numerically and depicted its solutions for $\tau < 5.5\pi$ and $\eta < 6.5\pi$ on a diagram, as shown in Fig. 4. Gray and black curves correspond to $\varepsilon = -1$ and $+1$, respectively, and dashed lines denotes arcs, which are parts of the primary orbit. The solutions of Eq. (4) give values of ε, τ, and η. The corresponding values of a, e, ε', and ε'' are uniquely determined from Eqs. (2) and (3) and from the second equation of Eq. (1).

Transfer time of generic arcs is free, and so the family presented on Hénon's diagram is continuous. Contrary to generic arcs, possible transfer times on odd arcs constitute a discrete set $2\tau = n\pi$, where n is an odd number. The appropriate set of these arcs can be easily found from the diagram using these transfer times.

Hénon's diagram considers the arcs with two different collisional points, whereas even arcs have coincident collision points (see Fig. 1a). They are not presented in the diagram. Even arcs obey a simple synchronism condition: the ratio of orbital periods of the

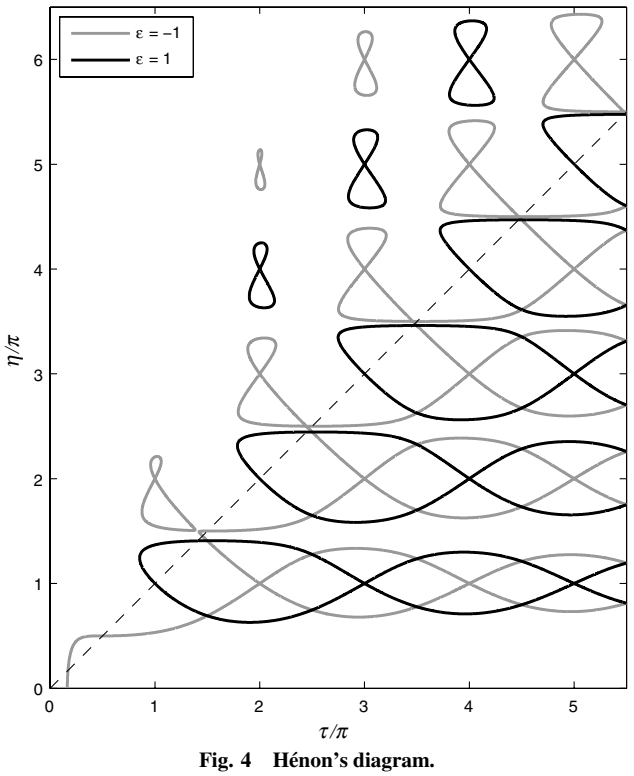

Fig. 4 Hénon's diagram.

primary and the spacecraft should be rational. From this condition, the semimajor axis is unambiguously defined as

$$a = (n/m)^{2/3} \tag{5}$$

where n and m are even numbers and denote, respectively, the half-revolutions of the primary and the spacecraft during the transfer. The two first equations of Eq. (1) imply

$$\varepsilon'' e = \frac{1 - 1/a}{\cos\eta} \tag{6}$$

Eccentric anomaly of the spacecraft is a free parameter. Thus, the even family is also continuous.

B. Periodic Trajectories

As stated at the beginning of the previous section, any arc in the 3BP with consecutive collisions is a periodic trajectory; that is, it may be continued periodically. Also, any combination of collisional trajectories with the same relative velocities at both ends is periodic. Matching of relative velocities is the essential condition to patch any set of collisional trajectories. We omit the other necessary condition restriction on the maximal turning angle at the present stage. Until this condition is not satisfied, we only have *potential candidates* for periodic trajectories.

The aim of this section is to develop a method for searching collisional arcs with the same relative velocities. Hénon's diagram helps with finding all such arcs. If a level line of relative velocity is drawn on Hénon's diagram, then the intersection of this line with Hénon's curves will give all collision arcs with this relative velocity.

Let us now derive a formula for calculating the relative velocity. The relative velocity vector is defined as $\mathbf{V}_\infty \triangleq \mathbf{V}_3 - \mathbf{V}_2$, where $\mathbf{V}_2$ and $\mathbf{V}_3$ are the velocity vectors of the primary and spacecraft, respectively, with respect to the central body. The equation of energy conservation can be written as

$$-\frac{\mu_1}{2a} = -\frac{\mu}{r} + \frac{(\mathbf{V}_2 + \mathbf{V}_\infty)^2}{2} \tag{7}$$

where μ_1 is the gravity constant of the central body, and r is the distance from the central body. The orbit of the primary is circular; therefore, $V_2^2 = \mu_1/r$. Rearranging Eq. (7) leads to

$$-\frac{V_\infty^2}{\mu_1} + \frac{3}{r} = 2\frac{\mathbf{V}_2 \cdot \mathbf{V}_3}{\mu_1} + \frac{1}{a} \tag{8}$$

To obtain the scalar product at the right side of Eq. (8), let us consider the scalar product of angular momentum vectors:

$$\mathbf{h}_2 \cdot \mathbf{h}_3 = (\mathbf{r} \times \mathbf{V}_2) \cdot (\mathbf{r} \times \mathbf{V}_3) = r^2(\mathbf{V}_2 \cdot \mathbf{V}_3) \tag{9}$$

Now $h_2 = \sqrt{r\mu_1}$ and $h_3 = \sqrt{p\mu_1}$, where p is the semilatus rectum of the spacecraft orbit. Therefore,

$$\mathbf{h}_2 \cdot \mathbf{h}_3 = \mu_1\sqrt{pr}\cos i \tag{10}$$

where i is the spacecraft orbit inclination. Comparing Eqs. (9) and (10) and substituting the result into Eq. (8) results in

$$-\frac{V_\infty^2}{\mu_1} + \frac{3}{r} = 2\sqrt{\frac{p}{r^3}}\cos i + \frac{1}{a} \tag{11}$$

In fact, the right side of Eq. (11) is Tisserand's criterion [15]. When $\cos i = \pm 1 = \varepsilon'$, Eqs. (2) and (3) enable the change of variables in Eq. (11), which finally gives

$$V_\infty = \sqrt{3 - 2\varepsilon'\sqrt{\frac{\sin^2\tau}{1 - \varepsilon\cos\tau\cos\eta}} - \frac{\sin^2\eta}{1 - \varepsilon\cos\tau\cos\eta}} \tag{12}$$

This is the implicit equation of the sought level lines in the same normalized variables as used by Hénon [11]. The intersection of curves from Eqs. (4) and (12) for a given V_∞ will provide solutions for arcs with the same relative velocity. For example, Fig. 5 presents solutions for such arcs with $V_\infty = 1$.

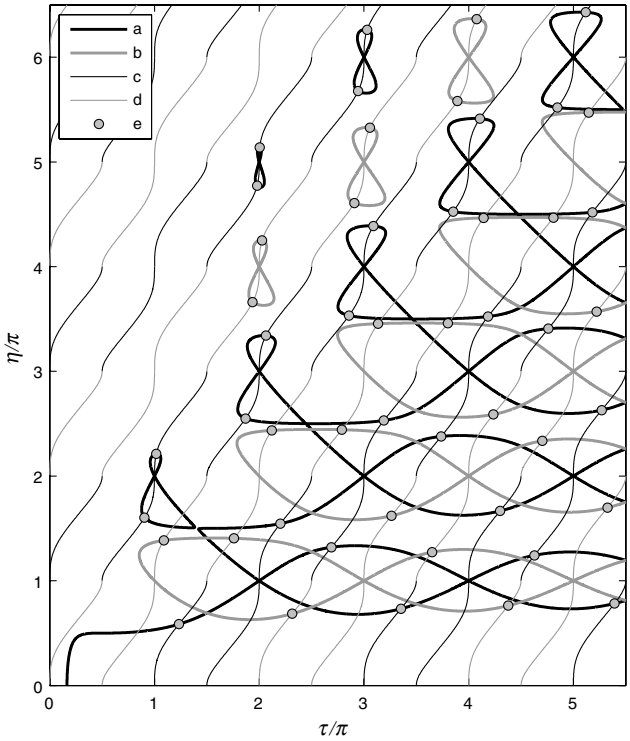

Fig. 5 Solutions for recursive arcs with $V_\infty = 1$. In the legend, a and b are recursive arcs for $\varepsilon = -1$ and $+1$, respectively; c and d are lines of equal relative velocity ($V_\infty = 1$) for $\varepsilon = -1$ and $+1$, respectively; and e denotes the solutions.

For odd arcs, $2\tau = n\pi$ (where n is odd); the inclination angle is free. Now Eq. (11) can be written as

$$V_\infty = \sqrt{3 - 2\cos i - \sin^2\eta} \tag{13}$$

Its analog for even arcs is

$$V_\infty = \sqrt{3 - 2\cos i\sqrt{\frac{2 - (m/n)^{2/3} - (n/m)^{2/3}\sin^2\eta}{\cos^2\eta}} - \left(\frac{m}{n}\right)^{2/3}} \tag{14}$$

Inclination of odd arcs is unambiguously defined by the relative velocity calculated from Eq. (12). Even arcs have one more degree of freedom; with relative velocity and resonance ratio fixed, inclination and eccentric anomaly are still free.

C. Concatenation of Collisional Arcs

As was previously discussed, a periodic trajectory can include several arcs patched together with gravity-assisted maneuvers. Every maneuver must meet the constraint on maximum turning angle of the velocity vector established by the planet mass and radius. The turning angle δ is given by [18]

$$\sin\frac{\delta}{2} = \frac{1}{1 + (\rho + h_p)V_\infty^2/\mu_2} \tag{15}$$

where V_∞ is the relative velocity; μ_2 and ρ are, respectively, the gravity constant and radius of the flyby planet; and h_p is the height of the hyperbola pericenter.

IV. Periodic Trajectories in the Circular 4BP

This section discusses a simple geometric method for identifying coplanar and out-of-plane transitional arcs. The method allows

obtaining periodic trajectories assembled from two transitional arcs and an arbitrary number of odd and even arcs.

A. Periodic Trajectories in the 4BP: Simple Case

Let us consider a system of a central body, two primaries, and a spacecraft under the following assumptions:

1) Primaries' orbits are circular and coplanar.

2) All transfer legs are the arcs with consecutive collisions.

3) Only one of the primaries can provide a sufficient gravity-assist maneuver to curve the spacecraft orbit.

The last assumption is justified when one of the planets has a sufficiently small mass and/or the pericenter of the flyby hyperbola is high enough. This simplified model is valid, for example, in one of the most studied problems today: the design of Earth–Mars *cyclers* [7–10,12–14]. Strict periodic motion in the true Earth–Mars system is impossible due to the considerable eccentricity of the Martian orbit and to the absence of orbital resonance between the Earth and Mars. A cycler does return periodically to a vicinity of Mars, but the vicinity is rather wide: its characteristic size is a few million kilometers, which is the same order of magnitude as the radius of Martian gravity sphere. This consideration is a sufficient justification of the accepted model.

Hénon's diagram was designed for the 3BP, yet it is efficient at predicting all periodic trajectories in the simplified two-planet system. In this section, we confine the study to periodic trajectories built from only one generic arc supplemented with an arbitrary number of odd and even arcs.

Any collisional trajectory can be repeated periodically in the two-planet system if the total transfer time is a multiple of the synodic year of the planet system:

$$2\tau + \frac{T_E}{2}\sum_j n_{E,j} = NT_{\text{syn}} \tag{16}$$

where 2τ is the transfer time on a generic orbit, T_E is Earth's orbital period, $T_{\text{syn}} = 1/(1/T_E - 1/T_M)$ is Earth–Mars synodic period (T_M is the Martian orbital period), $n_{E,j}$ is the number of Earth's half-revolutions during the jth even or odd arc, and N is a natural number. Let us denote, hereafter,

$$n_E \triangleq \sum_j n_{E,j}$$

Given N and n_E, we can point out a set of candidates for periodic trajectories using Hénon's diagram. The only additional condition is that one of the cycler's arcs must have an apoapsis above Mars's orbit to assure Mars encounters.

Figure 6 presents all possible solutions for generic arcs for $\{N, n_E\} = \{1, 0\}$ and $\{2, 3\}$. The figure shows that there are 11 and 13 solutions, respectively. When $n_E = 0$, the semimajor axis and eccentricity are readily obtained from Eqs. (2) and (3) using τ and η found in the graph. If $n_E \neq 0$, one can do the same with τ and η corrected in agreement with Eq. (16). Relative velocity at the collision is calculated using Eq. (12). If the set contains odd arcs, then their inclination can be calculated from Eq. (13), where η_j is obtained from Hénon's diagram for a chosen odd $n_{E,j}$. If the set contains even arcs, then, for a chosen resonance ($m_{E,j}$:$n_{E,j}$), either i or η_j is free. This freedom can be used to minimize the flyby turning angle.

Thus, a manifold of candidate cycler orbits can be found. Some candidates appear in earlier works as specific solutions to the Lambert problem. All of these cyclers (ballistic and near-ballistic, with periods of one, two, and three synodic years) are depicted in Fig. 6. The Aldrin cycler [6] has a period of one synodic year and solely contains a generic arc. It is a near-ballistic cycler because the required turning angle at the Earth flyby is about 15% above the maximal [12]. For the same reason, cycler $\{2, 3\}$ and $\{3, 1\}$ [the latter with two full revolutions on the generic arc (see Fig. 6)] are also near-ballistic. The cyclers $\{2, 1\}, \{3, 5\}$ (the latter with two full revolutions on the generic arc) are also near-ballistic, but due to a different reason: the apoapsis on these cyclers is slightly below Mars orbit.

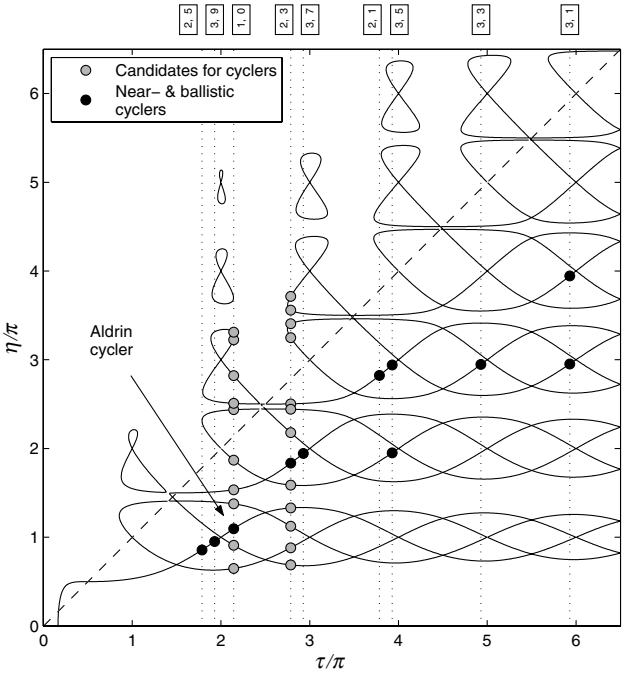

Fig. 6 Periodic trajectories in the Earth–Mars system (top labels are $\{N, n_E\}$).

However, cyclers $\{2, 5\}$, $\{3, 1\}$, and $\{3, 5\}$ (the latter with one full revolution on the generic arc) and cyclers $\{3, 3\}, \{3, 7\}$, and $\{3, 9\}$ are purely ballistic cyclers. All of these cyclers are described in more detail in [12].

B. Families of Recursive Trajectories

We will now extend the preceding proposed method to systems in which both planets are massive. Planetary orbits are assumed to be circular and coplanar. Hereafter a "P1 (P2) recursive trajectory" means the trajectory that originates from planet P1 (P2) and returns back to the same planet. Analogous terminology will be applied to arcs.

Every periodic trajectory contains one P1 recursive trajectory (see Fig. 7) and perhaps several odd and/or even P1 arcs. A recursive trajectory is similar to a recursive arc, but it can consist of several arcs: namely, two transitional arcs, P1 → P2 (first leg) and back (third leg), optionally supplemented with several P2 arcs (second leg) and P1 arcs (fourth leg). Legs 1 and 3 are essential, whereas legs 2 and 4 are optional. Relative velocities of both transitional arcs near P1 must be equal. Using Eq. (11), this condition can be written as

$$2\sqrt{\frac{p_1}{r_{\text{P1}}^3}}\cos i_1 + \frac{1}{a_1} = 2\sqrt{\frac{p_3}{r_{\text{P1}}^3}}\cos i_3 + \frac{1}{a_3} \tag{17}$$

where r_{P1} is the orbital radius of planet P1, and subindices at p, a, and i denote their relation to respective transitional arcs of legs 1 and 3. Analogously, relative velocities near P2 are also equal:

$$2\sqrt{\frac{p_1}{r_{\text{P2}}^3}}\cos i_1 + \frac{1}{a_1} = 2\sqrt{\frac{p_3}{r_{\text{P2}}^3}}\cos i_3 + \frac{1}{a_3} \tag{18}$$

where r_{P2} is the orbital radius of P2. In virtue of Eqs. (17) and (18), it implies

$$\sqrt{p_1}\cos i_1 = \sqrt{p_3}\cos i_3 \tag{19}$$

$$a_1 = a_3 \tag{20}$$

From Eqs. (19) and (20), it follows that if both transitional arcs are coplanar, then their eccentricities are equal as well. In addition, without losing generality, if transitional arcs of legs 1 and 3 are,

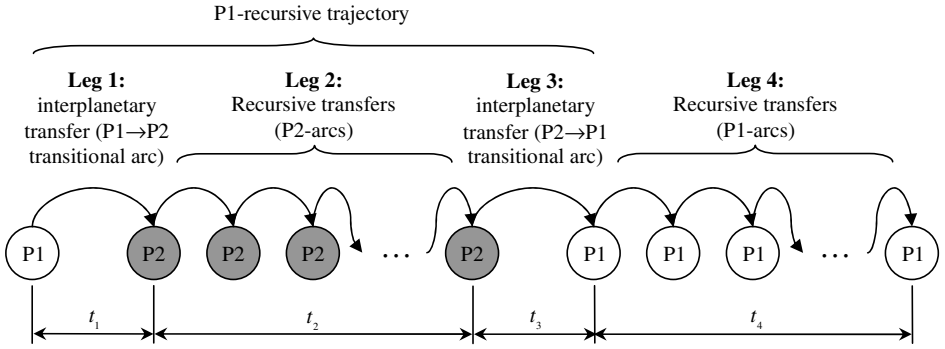

Fig. 7 Schematic representation of a cycler trajectory.

respectively, coplanar and noncoplanar, then it follows that [18]

$$p_3 = \frac{2r_{P1}r_{P2}}{r_{P1} + r_{P2}} \tag{21}$$

and, finally,

$$p_1 = \frac{2r_{P1}r_{P2}}{r_{P1} + r_{P2}}\cos^2 i_3 \tag{22}$$

To ease the navigation in the variety of periodic trajectories, they need classification. We will classify periodic trajectories considering only combinations of the two transitional arcs. Recall that the study is confined to the case when all loitering arcs belong to $k\pi$ type. Then at least one transitional arc must have an angular length other than $k\pi$, except for the case of resonant planetary systems.

As Table 1 suggests, there are four types of coplanar transitional arcs and two types of noncoplanar arcs. In total, they give 21 combinations of two transitional arcs (the order is not important). We sorted these combinations into five almost-disjointed classes, as presented in Tables 2 and 3 (there are some very particular cases that may belong to more than one class). Table 2 applies to any circular, coplanar, two-planet system: Table 3 applies to resonant systems only.

A number of examples of recursive arcs are shown in Fig. 8. Transitional arcs from the first class have the shape of recursive arcs, as shown in Fig. 8a. Combinations of {short, slow} and {long, fast} transitional arcs yield recursive arcs that start and end near the inner planet (case I.1 in Table 2). Combinations of {short, fast} and {long, slow} yield recursive arcs relative to the outer planet, as shown in Fig. 8b (case I.2 in Table 2).

Recursive trajectories from the second class are composed of transitional arcs from the same family (Fig. 8c). If the numbers of revolutions in both transitional arcs are equal, then the arcs are symmetric. In the third class, only one of the transitional arcs is coplanar (Fig. 8d). The fourth and fifth classes are only applicable in two-planet resonant systems, because we restrict ourselves to the second and the fourth legs, each having the total angular distance of $k\pi$. These are the peculiar orbits that are possible only in resonant systems. Classes IV and V comprise only these orbits. The orbits that do not meet this constraint are attributed to the first three classes.

C. Synchronization Condition of Recursive Trajectories in 4BP

Transfer angles of P1 and the spacecraft in a P1 recursive trajectory cannot differ but by $2\pi k$. Let us denote the transfer angle and time during each leg of the recursive trajectory by θ_j and t_j, respectively, j being the leg number ($j = 1, 2, 3$). During the second

Table 2 Recursive trajectories in a two-planet system

Class	Description	Transitional arcs	Remarks	Fig. no.
I.1	P1 is the inner planet, and P2 is the outer planet. The union of arcs is symmetric in the inner-planet synodic frame.	fast + long short + slow	Both transitional arcs are coplanar.	8a
I.2	P2 is the inner planet, and P1 is the outer planet. The union of arcs is symmetric in the outer-planet synodic frame.	short + fast slow + long	Both transitional arcs are coplanar.	8b
II	Both transitional arcs belong to the same family. The union of arcs is symmetric in both the inner and the outer synodic frames.	fast + fast slow + slow short + short long + long	Both transitional arcs are coplanar.	8c
III	The transfer angle of the noncoplanar transitional arc is $(2k-1)\pi$.	Any coplanar arc from the set (short, long, slow, fast) plus any noncoplanar arc from the set (slow, fast).	One transitional arc is coplanar, the other is noncoplanar.	8d

Table 3 Recursive trajectories in a resonant two-planet system

Class	Description	Transitional arcs	Remarks
IV	The combination of two transitional arcs is a closed orbit; its total transfer angle is $2\pi k$.	fast + slow short + long	Both transitional arcs are coplanar.
V	The transfer angle of each transitional arc is $(2k-1)\pi$.	Any noncoplanar arc from the set (slow, fast) plus any noncoplanar arc from the set (slow, fast).	Both transitional arcs are noncoplanar.

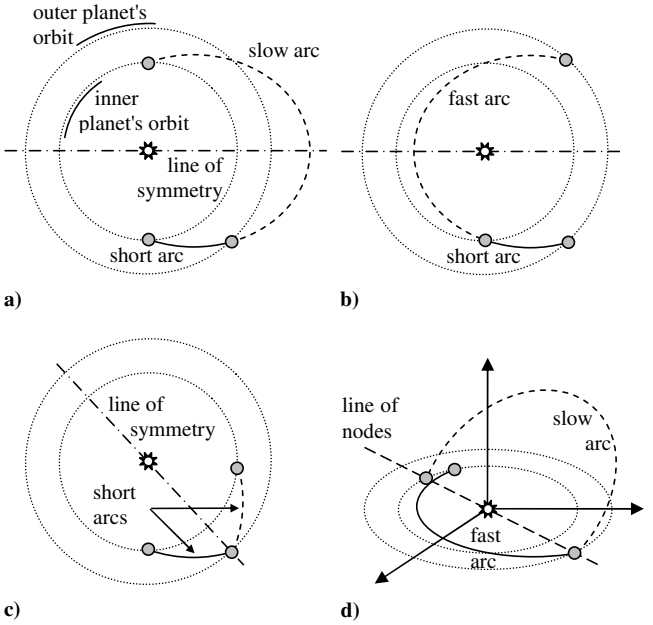

Fig. 8 Examples of recursive trajectories: a) class I.1 {short, slow}, b) class I.2 {short, fast}, c) class II {short, short}, and d) class III {fast coplanar, slow noncoplanar}.

leg, the spacecraft and P2 perform m_2 and n_2 half-revolutions, respectively. Therefore, the spacecraft transfer angle and time in the second leg can be written as $\theta_2 = m_2\pi$ and $t_2 = n_2 T_{P2}/2$, where T_{P2} is the orbital period of P2. Clearly,

$$\theta_1 + \theta_3 + m_2\pi = (t_1 + t_3 + 2\tau_2)\frac{2\pi}{T_{P1}} + 2\pi k \tag{23}$$

where $2\tau_2 \triangleq n_2 T_{P2}/2$. This is the general form of the synchronization condition for all classes of recursive trajectories. We shall use it further to obtain the respective recursive diagrams. Because of Eq. (20), $a_1 = a_3 = a$. Let us assume that the values k, m_2, n_2, T_{P1}, and T_{P2} are given and that $(a, \tilde{\theta}_1, \tilde{\theta}_3)$ is a solution to Eq. (23), with $\tilde{\theta}_3 > 2\pi k$. Then $(a, \tilde{\theta}_1 + 2\pi k, \tilde{\theta}_3 - 2\pi k)$ is again a solution.

In the following sections, a single recursive trajectory will represent the whole set. Hereafter, the units of length and time are always related with the Earth orbit.

D. Recursive Trajectories of Class I

Let us consider the synchronization problem for class-I trajectories containing legs 1, 2, and 3. Earth is P1 and Mars is P2 for class I.1, and vice versa for class I.2. Denoting $\theta_1 + \theta_3 = 2\theta_{13}$ and $t_1 + t_3 = 2t_{13}$, Eq. (23) implies

$$\theta_{13} + \frac{\pi}{2}m_2 = (t_{13} + \tau_2)r_{P1}^{-3/2} + \pi k \tag{24}$$

Without loss of generality, let us assume that the transfer angle of the first transitional arc is larger than that of the second arc. Starting from P1, after time t_{13}, the spacecraft will reach perihelion or aphelion (see case I.1 in Fig. 9). The coordinates of P1 and the spacecraft *at the beginning of motion* are

$$\begin{aligned} X &= r_{P1}\cos\theta_{13} = a(\cos\eta - \varepsilon'' e) \\ Y &= r_{P1}\sin\theta_{13} = \varepsilon' a\sqrt{1-e^2}\sin\eta \end{aligned} \tag{25}$$

In the same way, the time equation can be written as

$$t_{13} = a^{3/2}(\eta - \varepsilon'' e\sin\eta) \tag{26}$$

Using Eq. (24),

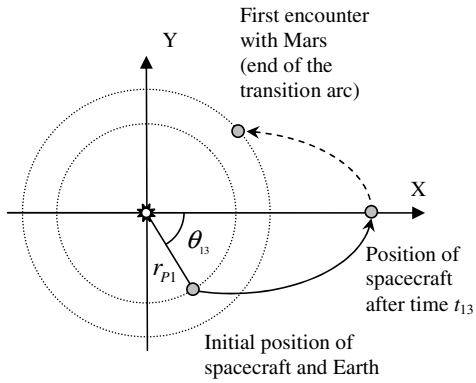

Fig. 9 Spacecraft's position at the beginning of motion, after time t_{13}, and at the first encounter with Mars.

$$\begin{aligned} \cos\theta_{13} &= \cos[(t_{13} + \tau_2)r_{P1}^{-3/2} - m_2\pi/2 + \pi k] \\ &= \cos(\tilde{\tau} + \pi k) = \varepsilon\cos\tilde{\tau} \end{aligned} \tag{27}$$

where

$$\varepsilon = \begin{cases} +1 \\ -1 \end{cases} \qquad \text{for } k \begin{cases} \text{even} \\ \text{odd} \end{cases}$$

and $\tilde{\tau}$ given by

$$\tilde{\tau} \triangleq (t_{13} + \tau_2)r_{P1}^{-3/2} - m_2\pi/2 \tag{28}$$

is *the extended half-time interval* (note that $\tilde{\tau}$ can be negative). Analogously,

$$\sin\theta_{13} = \varepsilon\sin\tilde{\tau} \tag{29}$$

Finally, the system of equations to be solved for a recursive trajectory is

$$\begin{cases} r_{P1}\cos\tilde{\tau} = \varepsilon a(\cos\eta - \varepsilon'' e) \\ r_{P1}\sin\tilde{\tau} = \varepsilon\varepsilon' a\sqrt{1-e^2}\sin\eta \\ (\tilde{\tau} + m_2\pi/2)r_{P1}^{3/2} - \tau_2 = a^{3/2}(\eta - \varepsilon'' e\sin\eta) \end{cases} \tag{30}$$

As in Sec. III.C,

$$a = r_{P1}\frac{1 - \varepsilon\cos\tilde{\tau}\cos\eta}{\sin^2\eta} \tag{31}$$

$$e = \frac{\varepsilon''\cos\eta - \varepsilon\varepsilon''\cos\tilde{\tau}}{1 - \varepsilon\cos\tilde{\tau}\cos\eta} \tag{32}$$

Now Eqs. (30–32) yield the synchronism condition for class-I trajectories:

$$\begin{aligned} &\sqrt{1 - \varepsilon\cos\tilde{\tau}\cos\eta}[\eta(1 - \varepsilon\cos\tilde{\tau}\cos\eta) - \sin\eta(\cos\eta - \varepsilon\cos\tilde{\tau})] \\ &\quad - (\tilde{\tau} + m_2\pi/2 - \tau_2 r_{P1}^{-3/2})|\sin^3\eta| = 0 \end{aligned} \tag{33}$$

It can be seen that without the second leg $r_{P1} = 1$, $\tilde{\tau} \equiv \tau$ and Eqs. (30–33) are identical to those obtained by Hénon [11] (see Sec. III.C). Therefore, solutions for periodic orbits presented in Hénon's diagram constitute only a particular case of this class.

Given two integers, n_2 and m_2, a recursive diagram for class I can be drawn using Eq. (33). Figures 10a and 10b present *all possible solutions* for the Earth–Mars system for recursive trajectories of class I.1 with $n_2 = m_2 = 1$ and class I.2 with $n_2 = m_2 = 2$, respectively. The second leg is a π-long P2 arc in class I.1 and either one 2π-long arc in 2:2 resonance or two π-long arcs in 1:1 resonance with P2 in class I.2.

Equation (28) provides $\tilde{\tau}$ for any specific t, n_2, and m_2. Then the corresponding diagrams will give appropriate sets of η and ε. Using

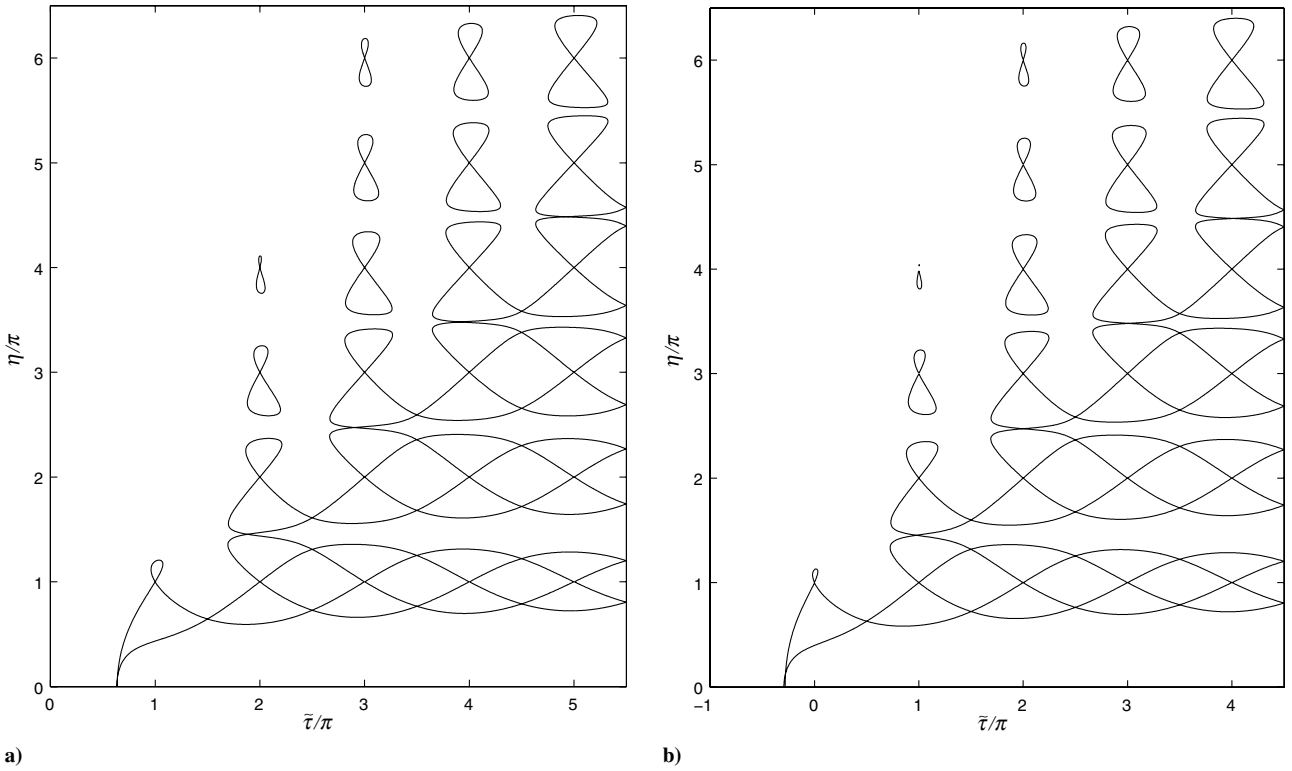

Fig. 10 Recursive diagrams: a) class I.1 for $n_2 = m_2 = 1$, b) class I.2 for $n_2 = m_2 = 2$.

these values, the values of a, e, ε', and ε'' are uniquely determined by Eqs. (31) and (32) and by the second equation of Eq. (30).

E. Recursive Trajectories of Class II

If both transitional arcs in a class-II trajectory count the same number of revolutions, then the transitional arcs are symmetric both in the sidereal frame (Fig. 8c) and in the synodic frames associated with P1 and P2. It is sufficient to consider only one arc and thus to reduce the number of timing equations from two to one.

The transitional arc for an arbitrary transitional angle may be described using Lagrange/Gibbs F and G functions [18]. If the initial position and velocity vectors $\mathbf{r}_1$ and $\mathbf{V}_1$ are given, then $\mathbf{r}_2$ and $\mathbf{V}_2$ are available from

$$\mathbf{r}_2 = F\mathbf{r}_1 + G\mathbf{V}_1 \qquad \mathbf{V}_2 = F_t\mathbf{r}_1 + G_t\mathbf{V}_1 \tag{34}$$

where

$$F = 1 - \frac{r_2}{p}(1-\cos\Delta f) = 1 - \frac{a}{r_1}(1-\cos\Delta E)$$

$$G = \frac{r_1 r_2}{h}\sin\Delta f = \Delta t - \sqrt{\frac{a^3}{\mu_1}}(\Delta E - \sin\Delta E)$$

$$F_t = \sqrt{\frac{\mu_1}{p}}\tan\frac{\Delta f}{2}\left(\frac{1-\cos\Delta f}{p} - \frac{1}{r_1} - \frac{1}{r_2}\right) = -\frac{\sqrt{\mu_1 a}}{r_1 r_2}\sin\Delta E$$

$$G_t = (1 + GF_t)/F \tag{35}$$

with Δt, Δf, and ΔE being the time, true anomaly, and eccentric anomaly intervals in the transitional arc, respectively.

Considering the synchronization condition [see Eq. (23)], let us denote $\theta_1 + \theta_3 = 2\tilde{\theta}_{13}$ and $t_1 + t_3 = 2\tilde{t}_{13}$ for recursive trajectories with an even total number of revolutions on legs 1 and 3, with $\theta_1 + \theta_3 = 2\tilde{\theta}_{13} + 2\pi$ and $t_1 + t_3 = 2\tilde{t}_{13} + 2\pi\sqrt{a^3/\mu_1}$ for the trajectories with an odd number of revolutions. With this notation,

$$\tilde{\theta}_{13} + \pi l + \frac{\pi}{2}m_2 = \tilde{t}_{13} + l\pi\sqrt{a^3} + \tau_2 + \pi k \tag{36}$$

where τ_2 is defined as in Sec. IV.C. A binary variable l is defined as 0 or 1 if the total number of full revolutions in legs 1 and 3 is an even or odd number, respectively.

The equation for the recursive diagram will be obtained using Eq. (35), in which $\Delta t = \tilde{t}_{13}$, $\Delta f = \tilde{\theta}_{13}$, and $\Delta E = \eta$, and $\sin\Delta f$ and $\cos\Delta f$ are to be calculated for direct and retrograde motion (see Fig. 11). Using Eq. (36),

$$\sin\Delta f = \varepsilon'\sin\tilde{\theta}_{13} = \varepsilon'\sin(\tilde{t}_{13} + l\pi\sqrt{a^3} + \tau_2 - \frac{\pi}{2}m_2 - \pi l + \pi k)$$
$$= \varepsilon'\sin(\tilde{\tau} - \pi l + \pi k) = \varepsilon\varepsilon'\varepsilon''\sin\tilde{\tau} \tag{37}$$

where

$$\varepsilon = \begin{cases} +1 \\ -1 \end{cases} \quad \text{for } k \begin{cases} \text{even} \\ \text{odd} \end{cases}$$

$$\varepsilon' = \begin{cases} +1 \\ -1 \end{cases} \quad \text{for} \begin{cases} \text{direct spaceraqft motion} \\ \text{retrograde spacecraft motion} \end{cases}$$

$$\varepsilon'' = \begin{cases} +1 \\ -1 \end{cases} \quad \text{for} \begin{cases} l = 0 \\ l = 1 \end{cases}$$

and $\tilde{\tau}$ is the extended half-time interval written for class II as

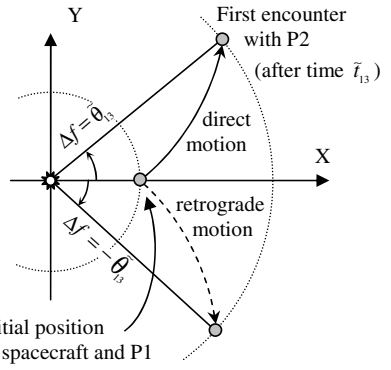

Fig. 11 Transfer angles at direct and retrograde motion of spacecraft.

$$\tilde{\tau} = \tilde{t}_{13} + l\pi\sqrt{a^3} + \tau_2 - \frac{\pi}{2}m_2 \tag{38}$$

Note that in class II, $\tilde{\tau}$ is defined as in class I, but written in a different way. Similarly,

$$\cos\Delta f = \varepsilon\varepsilon'' \cos\tilde{\tau} \tag{39}$$

Now, substituting Eqs. (37–39) and $\Delta E = \eta$ into Eq. (35), we get the equations

$$\begin{cases} \frac{R}{p}(1 - \varepsilon\varepsilon'' \cos\tilde{\tau}) = a(1 - \cos\eta) \\ \varepsilon\varepsilon'\varepsilon'' \frac{R}{\sqrt{p}} \sin\tilde{\tau} = \tilde{\tau} - \tau_2 + \frac{\pi}{2}m_2 - \sqrt{a^3}(\pi l + \eta - \sin\eta) \\ \frac{\varepsilon\varepsilon'\varepsilon'' \sin\tilde{\tau}}{1+\varepsilon\varepsilon'' \cos\tilde{\tau}} \left(\frac{1-\varepsilon\varepsilon'' \cos\tilde{\tau}}{p} - 1 - \frac{1}{R} \right) = -\frac{\sqrt{ap}}{R} \sin\eta \end{cases} \tag{40}$$

In this class, P1 is Earth and P2 is Mars; therefore, due to normalization, scaling the distances transforms r_{P1} to unit and r_{P2} to R. From Eq. (40), a and p are available:

$$a = z/z_\eta \tag{41}$$

$$p = Rz_\tau/z \tag{42}$$

where

$$z_\tau \triangleq 1 - \varepsilon\varepsilon'' \cos\tilde{\tau} \qquad z_\eta \triangleq 1 - \cos\eta$$
$$z \triangleq 1 + R - \varepsilon\varepsilon'\varepsilon'' \sqrt{R/(z_\tau z_\eta)} \sin\eta \sin\tilde{\tau}$$

In virtue of Eqs. (40–42), the synchronization equation is

$$\varepsilon\varepsilon'\varepsilon'' \sin\tilde{\tau} \sqrt{Rzz_\eta^3} + (\pi l + \eta - \varepsilon'' \sin\eta)\sqrt{z_\tau z^3} - \left(\tilde{\tau} - \tau_2 + \frac{\pi}{2}m_2\right)\sqrt{z_\tau z_\eta^3} = 0 \tag{43}$$

Figure 12 presents examples of diagrams for recursive trajectories in the Earth–Mars system with $n_2 = m_2 = 0$ (Figs. 12a–12c) and $n_2 = m_2 = 2$ (Fig. 12d).

It should be remarked that the recursive diagram of class-II forms infinitely many analytic curves. Actually, their number is twice as large as those in Hénon's diagram (there are twice more families of recursive trajectories in class II than recursive arcs). In addition, it can be seen from the figures that ε and ε'' do not change their values along the curves, but ε' does.

Implementation of the proposed method looks very similar in application to classes I and II. Given $t_1 + t_3$ and the resonance ratio n_2:m_2, the extended time $\tilde{\tau}$ can be calculated using Eq. (38) with $\tilde{t}_{13} + l\pi\sqrt{a^3} = (t_1 + t_3)/2$. The appropriate sets of η, ε, ε', and ε''

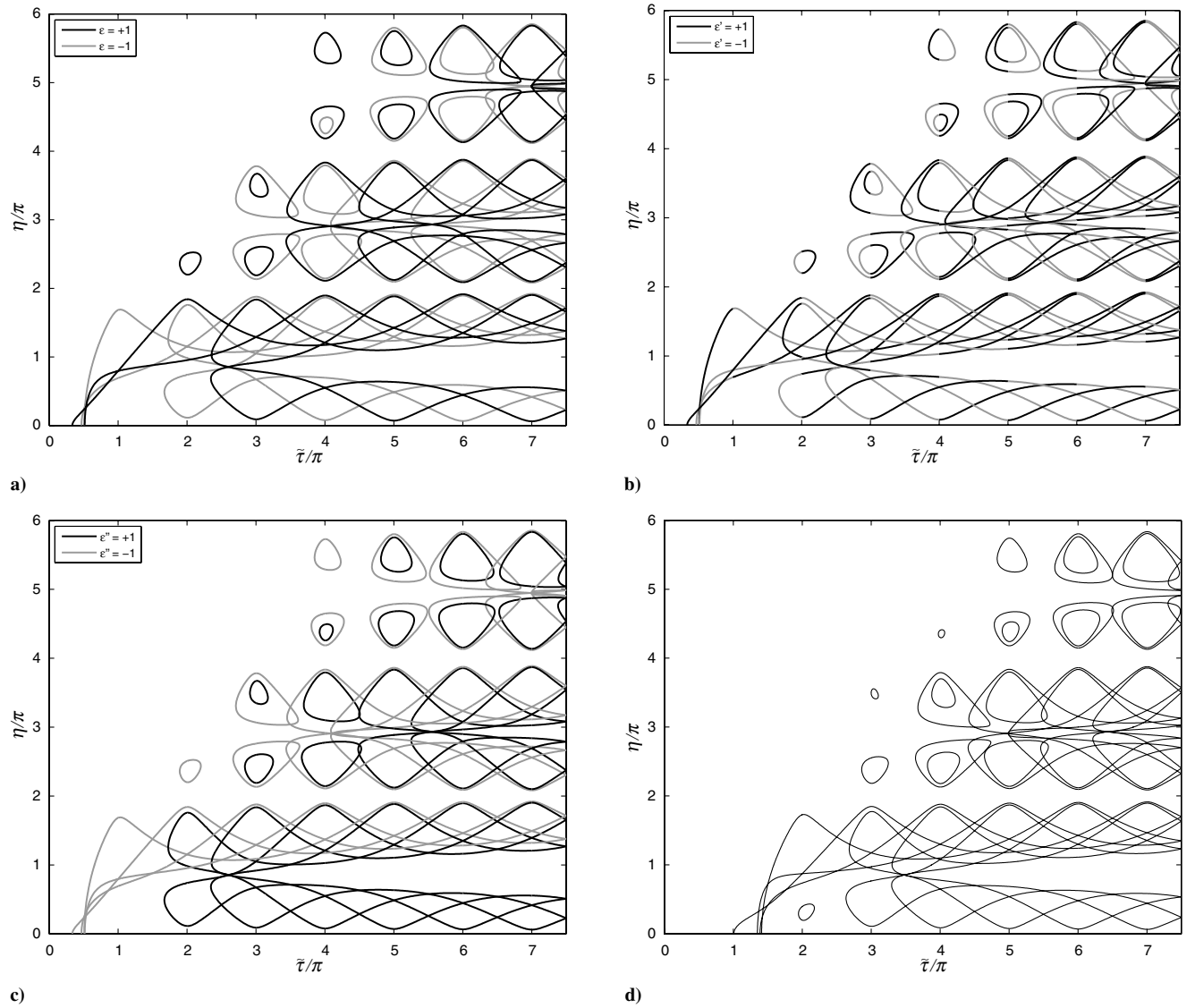

Fig. 12 Recursive diagrams for class II: a, b, c) diagrams for $n_2 = m_2 = 0$, d) for $n_2 = m_2 = 2$.

are present in the corresponding recursive diagrams. The values of a and e are uniquely determined from Eqs. (41) and (42), respectively.

F. Recursive Trajectories of Class III

Without losing generality, let us assume that leg 1 (P1 → P2) is coplanar and that leg 3 (P2 → P1) is not. As agreed, P1 is Earth, and units are normalized to the Earth orbit. In class III, $p_1 \neq p_3$ though $a_1 = a_3 = a$ [see Eqs. (20–22)]. Therefore, the orbital and time equations for the two legs must be solved separately.

The transfer angle of noncoplanar arcs cannot differ from $\theta_3 = (2k_3 + 1)\pi$. Thus,

$$\theta_1 = 2\tilde{\tau} + \tilde{k}\pi \tag{44}$$

where $\tilde{k} \triangleq 2k - 2k_3 - 1$. The extended half-time interval $\tilde{\tau}$ has the same meaning as in classes I and II, and it is written for this case as

$$\tilde{\tau} = t_{13} + \tau_2 - m_2\pi/2 \tag{45}$$

The two continuous parameters for the synchronization equation are $\tilde{\tau}$ and η_1. The trajectory with $k_3 = 0$, and therefore $\theta_3 = \pi$ represents the respective family.

Equations (34) and (35) are valid for any type of transitional arc. Applying these to class III, we obtain the same system of equations as Eq. (40), but now ε is always unity, due to Eq. (44), $\tilde{k} = 2k - 1$, and $\varepsilon'' = 0$. Thus, Eqs. (41) and (42) are valid, but

$$z_\tau \triangleq 1 + \cos(2\tilde{\tau}) \qquad z_\eta \triangleq 1 - \cos\eta_1$$
$$z \triangleq 1 + R + \varepsilon'\sqrt{R/(z_\tau z_\eta)}\sin\eta_1 \sin(2\tilde{\tau})$$

Thus, the transfer time for leg 1 is

$$t_1 = -\varepsilon'\frac{R}{\sqrt{p_1}}\sin(2\tilde{\tau}) + \sqrt{a^3}(\eta_1 - \sin\eta_1) \tag{46}$$

The orbital parameters for the noncoplanar transitional arc are

$$a = \frac{1 + R}{1 - \cos\eta_3} \tag{47}$$

$$p_3 = \frac{2R}{1 + R} \tag{48}$$

$$t_3 = \sqrt{a^3}(\eta_3 - \sin\eta_3) \tag{49}$$

From Eqs. (41) and (47), the eccentric anomaly interval in the noncoplanar transitional arc is

$$\eta_3 = \begin{cases} \alpha \\ 2\pi - \alpha \end{cases} \quad \text{for} \quad \begin{cases} \text{fast transitional arc} \\ \text{slow transitional arc} \end{cases} \tag{50}$$

where

$$\alpha = \arccos[1 - (1 + R)z_\eta/z]$$

Finally, the synchronization equation for class III can be written as

$$\varepsilon'\sqrt{Rzz_\eta^3}\sin(2\tilde{\tau}) - (\eta_1 - \sin\eta_1 + \eta_3 - \sin\eta_3)\sqrt{z_\tau z^3}$$
$$+ (2\tilde{\tau} - 2\tau_2 + \pi m_2)\sqrt{z_\tau z_\eta^3} = 0 \tag{51}$$

In addition, the inclination of the noncoplanar transitional arc is

$$\cos i_3 = \sqrt{\frac{z_\tau(1 + R)}{2z}} \tag{52}$$

However, now not all solutions depicted in the diagram (see, for example, Fig. 13) are feasible. Indeed, $\tilde{\tau}$ and η_1 can meet Eq. (51), but η_3 or inclination can turn out complex. The solutions offered by the diagram need a validity check.

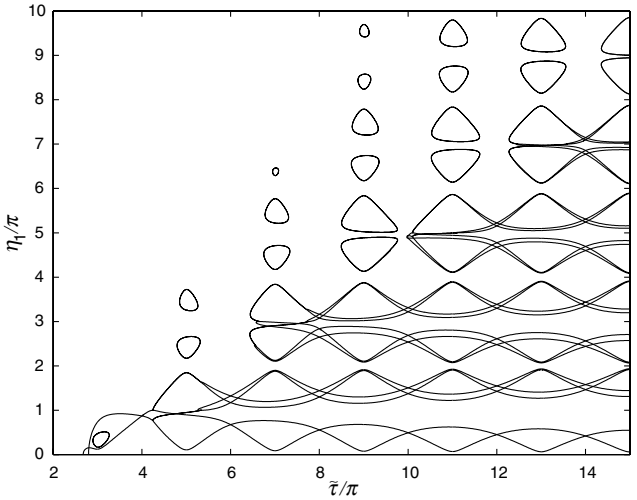

Fig. 13 Recursive diagram for class III for $n_2 = m_2 = 2$.

G. Predicting Periodic Trajectories from Recursive Diagrams

The method of predicting periodic trajectories in 4BP, in which both planets provide gravity-assisted maneuvers, is identical to that described in Sec. IV.A, with the recursive arcs replaced by recursive trajectories. When both planets enable gravity-assist maneuvers, every recursive generic arc can be replaced by a recursive trajectory with intermediate encounters with P2. The problem to be solved is synchronization of recursive trajectories.

Hereafter, a cycler trajectory is supplemented with the fourth leg, which consists of an arbitrary number of P1 arcs. Because the period of the cycler is NT_{syn}, the following equation is valid:

$$t_1 + t_2 + t_3 + t_4 = NT_{\text{syn}} \tag{53}$$

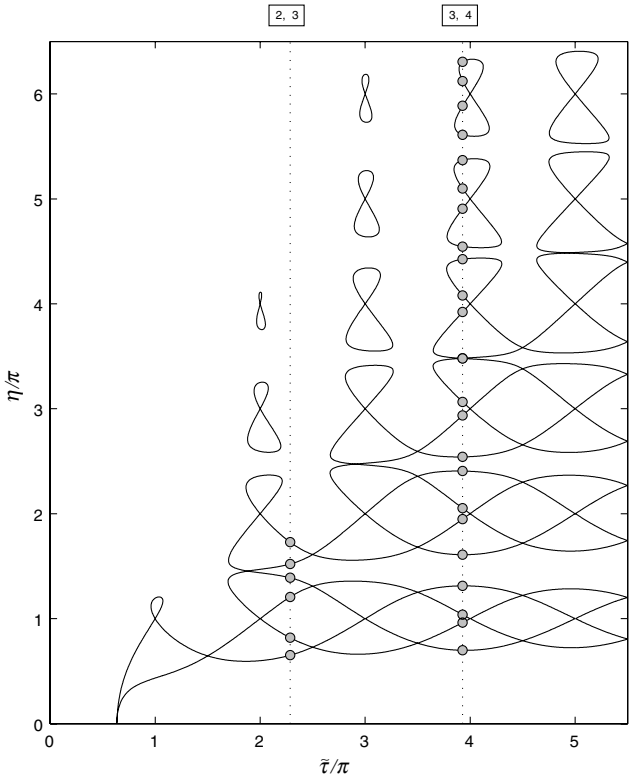

Fig. 14 Candidates for periodic trajectories in the Earth–Mars system for class I.1 with $n_2 = m_2 = 1$, top labels are $\{N, n_4\}$.

Table 4 Purely ballistic two-synodic periodic trajectory of class III

Heliocentric orbit elements						Flyby elements	
Leg no.	Arc no.	a, AU	e	i, deg	θ, deg	V_∞, km/s	Heights of the hyperbolic passage, km
1	1	1.3	0.284	0	93.54	5.7	7617
3	2	1.3	0.269	5.3	540	6.2	2655
4	3	1	0	12	180	5.7	2834
4	4	1	0.16	7.6	360	5.7	7617

where t_j is the duration of leg j ($j = 1, 2, 3, 4$). With $t_2 = 2\tau_2$ and $t_4 = 2\tau_4$, the transfer times are defined by nonnegative integers n_4 and n_2, which are the numbers of half-revolutions with respect to P1 and P2, as $2\tau_4 = n_4 T_{\mathrm{P1}}/2$ and $2\tau_2 = n_2 T_{\mathrm{P2}}/2$. For example, considering periodic trajectories of class I.1,

$$2t_{13} + 2\tau_2 + 2\tau_4 = NT_{\mathrm{syn}} \tag{54}$$

From Eqs. (28) and (54), it follows that

$$\tilde{\tau} = NT_{\mathrm{syn}}/2 - \tau_4 - m_2\pi/2 \tag{55}$$

where m_2 is the number of the spacecraft's total half-revolutions during all odd and even arcs relative to P2 (leg two). Using this strategy, candidate cyclers presented in Fig. 14 were found. These are the trajectories of class I.1 in the Earth–Mars system with $n_2 = m_2 = 1$ for $\{N, n_4\} = \{2, 3\}$ and $\{3, 4\}$.

In conclusion, Table 4 and Fig. 15 present an example of a purely ballistic class-III cycler in the system of massive Earth and Mars. Its period is two synodic years and the Earth-to-Mars transfer time is 134 days. The final flyby hyperbolic elements correspond to the arc beginning. The orbital period of Mars was assumed [13] as 2.13 years. Leg 2 is absent. The gravity of Mars is used to change inclination of the spacecraft's trajectory.

V. Conclusions

In this paper, we propose a new technique for generating periodic passive interplanetary trajectories in a circular coplanar system with two planets. It yields the manifold of these trajectories, including coplanar and noncoplanar interplanetary passages. Periodic trajectories (cyclers) are predicted under the approximation of collisional trajectories. The method expands Hénon's [11] study of collisional trajectories in the three-body problem and inherits its major merits: explicit analytical description of the manifold, suitable for analytical and numerical investigation, and the possibility of its comprehensible graphical presentation, which helps with clearing up the set of sought solutions and avoidance of their omission.

Every periodic trajectory with consecutive gravity-assisted maneuvers can be divided into sequential recursive trajectories. They were classified into five classes, three of them existent in any two-planetary system and the remaining two only in resonant systems. Relevant equations were presented for each class. Hénon's [11] solutions were found applicable to the study of periodic trajectories in the four-body problem. The manifold of sought periodic trajectories may be presented in a diagram similar to Hénon's diagram.

The method covers the case with both planets massive. When applied to the idealized (coplanar circular) Earth–Mars system, it enabled the discovery of a variety of new cyclers in addition to the orbits known from earlier works, which were constrained to distant Mars flybys and neglected the Martian perturbations of the orbit. Future work will deal with synchronization problems of recursive trajectories of various classes, including any number of generic returns to both planets.

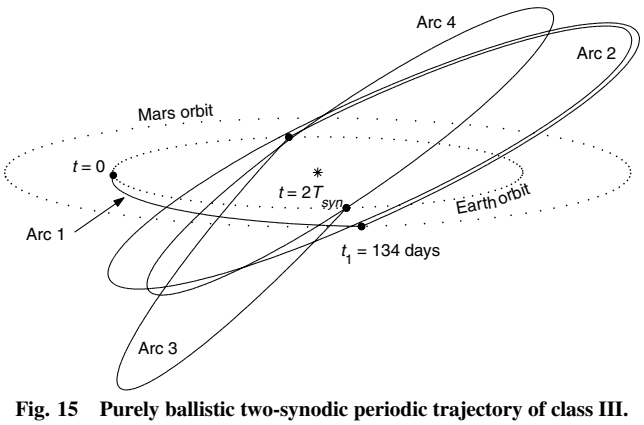

Fig. 15 Purely ballistic two-synodic periodic trajectory of class III.

References

[1] Hollister, W. M., "Periodic Orbits for Interplanetary Flight," *Journal of Spacecraft and Rockets*, Vol. 6, No. 4, 1969, pp. 366–369.
[2] Menning, M. D., "Freefall Periodic Orbits Connecting Earth and Venus," M.Sc. Thesis, Dept. of Aeronautics and Astronautics, Massachusetts Inst. of Technology, Cambridge, MA, July 1968.
[3] Rall, C. S., "Freefall Periodic Orbits Connecting Earth and Mars," Ph.D. Dissertation, Dept. of Aeronautics and Astronautics, Massachusetts Inst. of Technology, Cambridge, MA, Oct. 1969.
[4] Niehoff, J., "Pathways to Mars: New Trajectory Opportunities," *American Astronautical Society*, Paper 86-172, July 1986.
[5] Niehoff, J., Friedlander, A., and McAdams, J., "Earth–Mars Transport Cycler Concepts," *International Astronautical Congress*, Paper 91-438, Oct. 1991.
[6] Byrnes, D. V., Longuski, J. M., and Aldrin, B., "Cycler Orbit Between Earth and Mars," *Journal of Spacecraft and Rockets*, Vol. 30, No. 3, 1993, pp. 334–336.
[7] McConaghy, T. T., Longuski, J. M., and Byrnes, D. V., "Analysis of a Broad Class of Earth–Mars Cycler Trajectories," AIAA Paper 2002-4420, Aug. 2002.
[8] McConaghy, T. T., Yam, C. H., Landau, D. F., and Longuski, J. M., "Two-Synodic-Period Earth–Mars Cyclers with Intermediate Earth Encounter," American Astronautical Society, Paper 03-509, Aug. 2003.
[9] Byrnes, D. V., McConaghy, T. T., and Longuski, J. M., "Analysis of Various Two Synodic Period Earth–Mars Cycler Trajectories," AIAA Paper 2002-4423, Aug. 2002.
[10] Patel, M. R., Longuski, J. M., and Sims, J. A., "Mars Free Return Trajectories," *Journal of Spacecraft and Rockets*, Vol. 35, No. 3, 1998, pp. 350–354.
[11] Hénon, M., "Sur les Orbites Interplanétaires qui Recontrent Deux Fois la Terre," *Bulletin Astronomique*, Series 3.3, 1968, pp. 377–402.
[12] Russell, R. P., and Ocampo, C. A., "Systematic Method for Constructing Earth–Mars Cyclers Using Free-Return Trajectories," *Journal of Guidance, Control, and Dynamics*, Vol. 27, No. 3, 2004, pp. 321–335.
[13] Russell, R., and Ocampo, C., "Global Search for Idealized Free-Return Earth–Mars Cyclers," *Journal of Guidance, Control, and Dynamics*, Vol. 28, No. 2, 2005, pp. 194–208.
[14] Russell, R., and Ocampo, C., "Optimization of a Broad Class of Ephemeris Model Earth–Mars Cyclers," *Journal of Guidance, Control, and Dynamics*, Vol. 29, No. 2, 2006, pp. 354–367.
[15] Szebehely, V. G., *Theory of Orbits, The Restricted Problem of Three Bodies*, Academic Press, New York, 1967, pp. 26–34, 49, 583.
[16] Poincaré, H., *Les Méthodes Nouvelles de la Mécanique Céleste, Tome 3*, Gauthier-Villars, Paris, 1899, pp. 362–371.
[17] Bruno, A. D., *The Restricted 3-Body Problem: Plane Periodic Orbits*, Walter de Gruyter, Berlin, 1994, Part 2, pp. 114–133.
[18] Battin, R. H., *An Introduction to the Mathematics and Methods of Astrodynamics*, Revised Edition, AIAA, Reston, VA, 1999, pp. 128–130, 162–164, 241, 429.